

Observation of a fine structure in $e^+e^- \rightarrow \text{hadrons}$ production at the nucleon-anti-nucleon threshold

R.R. Akhmetshin^{1,2}, A.N. Amirkhanov^{1,2}, A.V. Anisenkov^{1,2}, V.M. Aulchenko^{1,2}, V.Sh. Banzarov¹, N.S. Bashtovoy¹, D.E. Berkaev^{1,2}, A.E. Bondar^{1,2}, A.V. Bragin¹, S.I. Eidelman^{1,2,5}, D.A. Epifanov^{1,2}, L.B. Epshteyn^{1,2,3}, A.L. Erofeev^{1,2}, G.V. Fedotov^{1,2}, S.E. Gayazov^{1,2}, A.A. Grebenuk^{1,2}, S.S. Gribanov^{1,2}, D.N. Grigoriev^{1,2,3}, F.V. Ignatov^{1,2}, V.L. Ivanov^{1,2}, S.V. Karpov¹, V.F. Kazanin^{1,2}, I.A. Koop^{1,2}, A.N. Kirpotin¹, A.A. Korobov^{1,2}, A.N. Kozyrev^{1,3}, E.A. Kozyrev^{1,2}, P.P. Krokovny^{1,2}, A.E. Kuzmenko^{1,2}, A.S. Kuzmin^{1,2}, I.B. Logashenko^{1,2}, P.A. Lukin^{1,2}, K.Yu. Mikhailov¹, V.S. Okhapkin¹, A.V. Otboev¹, Yu.N. Pestov¹, A.S. Popov^{1,2}, G.P. Razuvaev^{1,2}, A.A. Ruban¹, N.M. Ryskulov¹, A.E. Ryzhenkov^{1,2}, A.I. Senchenko¹, Yu.M. Shatunov¹, P.Yu. Shatunov¹, V.E. Shebalin^{1,2}, D.N. Shemyakin^{1,2}, B.A. Shwartz^{1,2}, D.B. Shwartz^{1,2}, A.L. Sibidanov^{1,4}, E.P. Solodov^{1,2}, A.A. Talyshchev^{1,2}, V.M. Titov¹, S.S. Tolmachev^{1,2}, A.I. Vorobiov¹, I.M. Zemlyansky¹, and Yu.V. Yudin^{1,2}

1. *Budker Institute of Nuclear Physics, SB RAS, Novosibirsk, 630090, Russia*

2. *Novosibirsk State University, Novosibirsk, 630090, Russia*

3. *Novosibirsk State Technical University, Novosibirsk, 630092, Russia*

4. *University of Victoria, Victoria, BC, Canada V8W 3P6*

5. *Lebedev Physical Institute, RAS, Moscow, 119333, Russia*

(Dated: November 21, 2018)

A study of hadron production at the nucleon-antinucleon threshold has been performed with the CMD-3 detector at the VEPP-2000 e^+e^- collider. A very fast rise with about 1 MeV width has been observed in the $e^+e^- \rightarrow p\bar{p}$ cross section. A sharp drop in the $e^+e^- \rightarrow 3(\pi^+\pi^-)$ cross section has been confirmed and found to have a less than 2 MeV width, in agreement with the observed fast rise of the $e^+e^- \rightarrow p\bar{p}$ cross section. For the first time a similar sharp drop is demonstrated in the $e^+e^- \rightarrow K^+K^-\pi^+\pi^-$ cross section. The behavior of the $e^+e^- \rightarrow 3(\pi^+\pi^-)$, $K^+K^-\pi^+\pi^-$ cross sections cannot be explained by an interference of any resonance amplitude with continuum, therefore this phenomenon cannot be due to a narrow near-threshold resonance. No such structure has been observed in the $e^+e^- \rightarrow 2(\pi^+\pi^-)$ cross section.

PACS numbers: 13.66.Bc, 14.40.Cs, 13.25.Gv, 13.25.Jx, 13.20.Jf

I. INTRODUCTION

Production of six pions in e^+e^- annihilation, studied at DM2 [1–3], showed a “dip” in the cross section at about 1.9 GeV, confirmed later by the Fermilab E831 experiment in photoproduction [4, 5], and with a much larger effective integrated luminosity at BaBar [6] using initial-state radiation (ISR). Even earlier, a narrow structure near the proton-antiproton threshold has been also observed in the total cross section of e^+e^- annihilation into hadrons in the FENICE experiment [7]. A measurement of the CMD-3 Collaboration [8] confirmed these observations and demonstrated that the drop in the $e^+e^- \rightarrow 3(\pi^+\pi^-)$ cross section occurred in the narrow energy range of less than 10 MeV width. The origin of the “dip” remains unclear, but one of the explanations suggests the presence of a below-threshold proton-antiproton ($p\bar{p}$) resonance [9]. Alternatively, in Ref. [10–13] the “dip” is due to the strong interaction

in virtual nucleon-antinucleon ($N\bar{N}$) production, and is related to the fast rise of the $e^+e^- \rightarrow N\bar{N}$ cross section and $N\bar{N}$ annihilation to hadrons. This hypothesis is supported by the fast increase of the $p\bar{p}$ [14, 15] and $n\bar{n}$ [16] form factors near threshold, and explains a similar drop in the $\eta'(958)\pi^+\pi^-$ spectrum, observed by the BES-III Collaboration in the $J/\psi \rightarrow \eta'(958)\pi^+\pi^-\gamma$ decay [17]. The authors of Ref. [10] consider the two-step process $e^+e^- \rightarrow N\bar{N} \rightarrow \text{multipions}$ and evaluate the total reaction amplitude for various intermediate mechanisms of the $e^+e^- \rightarrow 5\pi, 6\pi$ reactions. In Refs. [11–13] the authors go even further taking into account the proton-neutron mass difference and $p\bar{p}$ Coulomb interaction.

However, the mass-energy resolution of the previous experiments does not allow a study of the fine structure of the “dip” or the rise of the $e^+e^- \rightarrow N\bar{N}$ cross section. In this paper we present the analysis of the data sample based on 50 pb⁻¹ of integrated luminosity collected with the CMD-3 detector [18] in the 1.5–2.0 GeV center-

of-mass energy ($E_{c.m.}$) range. These data were collected in an energy scan at 29 c.m. energy points, performed at the VEPP-2000 collider with the upgraded injection complex [19–22]. The scan of the $N\bar{N}$ -threshold energy range was performed with a fine step, corresponding to the c.m. energy spread. The beam energy and energy spread have been monitored by the back-scattering-laser-light system [23, 24], providing an absolute energy measurement with better than 0.1 MeV uncertainty in every single measurement. During data taking the $E_{c.m.}$ variations around a central value did not exceed 0.1 MeV at each energy point: this value is taken as the systematic uncertainty estimate. The energy spread, $\sigma_{E_{c.m.}}$, is measured to be 0.95 ± 0.10 MeV at the $N\bar{N}$ threshold: the added uncertainty is our estimate of a systematic effect with a negligible contribution of the statistics.

The luminosity was measured using events of Bhabha scattering at large angles [25].

II. THE $e^+e^- \rightarrow 3(\pi^+\pi^-)$ CROSS SECTION

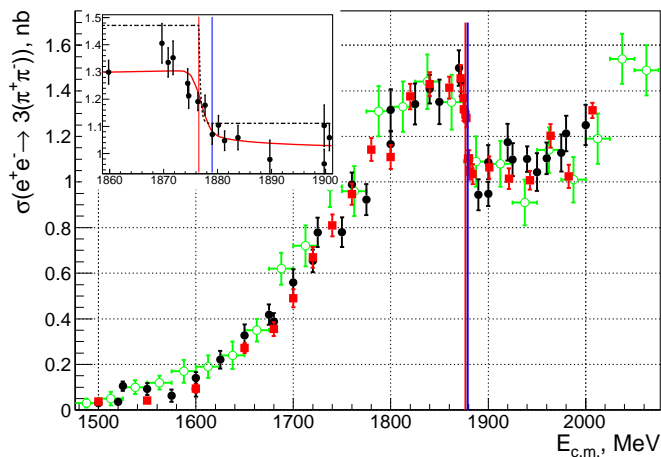


FIG. 1: The $e^+e^- \rightarrow 3(\pi^+\pi^-)$ Born cross section measured with the CMD-3 detector in the 2017 run (squares). The results of the previous CMD-3 measurement [8] are shown by dots and those of BaBar [6] by open circles. The inset shows the visible cross section with the fit described in the text. The vertical lines show the $N\bar{N}$ thresholds.

The analysis of the $e^+e^- \rightarrow 3(\pi^+\pi^-)$ process was de-

scribed in detail in Ref. [8]. For the new data we have reproduced all steps for selection of five and six charged tracks, and the calculation of the efficiency and radiative corrections. As in Ref. [8], we have a background-free sample of the six-track signal events, and use the ratio of the five- and six-track events to correct the efficiency. With the new data sample, the number of signal events with six charged tracks increased to 10155 (compared to 2887 events in the previous analysis) and that with one missing track to 17822 (5069) events. The cross section obtained from the new data is shown in Fig. 1 by squares, while the BaBar [6] and previous CMD-3 [8] data are shown by open and closed circles, respectively. Our previous result is confirmed with better statistical accuracy, while a systematic uncertainty is estimated at the same 6% level, mostly dominated by the uncertainties in the efficiency and background estimate. The “dip” at the $N\bar{N}$ threshold is also confirmed and is studied in more detail (see below).

III. THE $e^+e^- \rightarrow K^+K^-\pi^+\pi^-$ CROSS SECTION

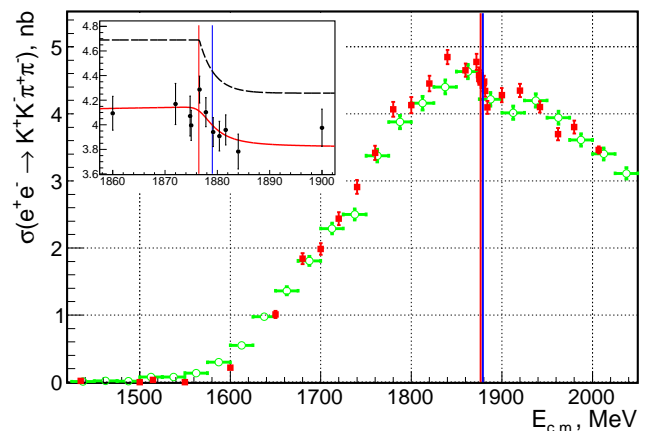


FIG. 2: The $e^+e^- \rightarrow K^+K^-\pi^+\pi^-$ Born cross section measured with the CMD-3 detector in the 2017 run (squares). The results of the BaBar [27] measurements are shown by open circles. The inset shows the visible cross section with the fit described in the text. The vertical lines show the $N\bar{N}$ thresholds.

The analysis of the $e^+e^- \rightarrow K^+K^-\pi^+\pi^-$ process was

described in detail in Ref. [26]. For the new data we have reproduced all steps for selection of four charged tracks, pion-kaon separation procedure, and the calculation of the efficiency and radiative corrections. A specially designed likelihood function is used to separate kaons and pions. In this analysis we use events with exactly four charged tracks which have practically no background. The events with one missing kaon or events with a missing pion are not used to reduce the uncertainty in the background subtraction. Nevertheless, the same overall statistical accuracy is achieved since the scan around the $N\bar{N}$ threshold is performed with large integrated luminosity that allows us to select about 1500 signal events per energy point. The cross section obtained from the new data is shown in Fig. 2 by squares, while the BaBar [27] data are shown by open circles. Our previous result is confirmed with better statistical accuracy, while a systematic uncertainty remains at the same 6% level, dominated by uncertainty in the efficiency estimate. A statistically significant “dip” at the $N\bar{N}$ threshold is observed for the first time in this channel, and is studied in more detail below.

IV. THE $e^+e^- \rightarrow p\bar{p}$ CROSS SECTION AT THE $N\bar{N}$ THRESHOLD

The analysis procedure is described in our previous publication [15]. At the energies near threshold, for $E_{c.m.} < 1900$ MeV, protons and antiprotons from the reaction $e^+e^- \rightarrow p\bar{p}$ stop in the material of the beam pipe because of very low momentum. To select such events, we look for the products of antiproton annihilation with more than two charged tracks coming from the aluminum beam pipe. Comparison of the calorimeter response for such events below and above the $N\bar{N}$ threshold yields the number of $p\bar{p}$ events. Points below the production thresholds, where we assume no signal from the $e^+e^- \rightarrow p\bar{p}$ reaction, are used for background normalization and we obtain 490 ± 30 signal events in the energy range from the production threshold to 1900 MeV.

Starting from $E_{c.m.} = 1900$ MeV, protons have enough energy to penetrate the beam pipe, and above this energy no annihilation of antiprotons at the beam pipe is observed. Protons and antiprotons are detected as collinear tracks with large specific energy losses, dE/dx , in the drift chamber (DC) of the CMD-3: we detect 4770 signal events. At each energy a visible cross section is calculated as the number of selected events divided by the detection efficiency and integrated luminosity. The obtained $e^+e^- \rightarrow p\bar{p}$ visible cross section is shown in Fig. 3. We estimate the systematic uncertainty as about 10%, dominated by the uncertainty in the efficiency calculation: a special study was performed to estimate data-MC difference in the reconstruction efficiency.

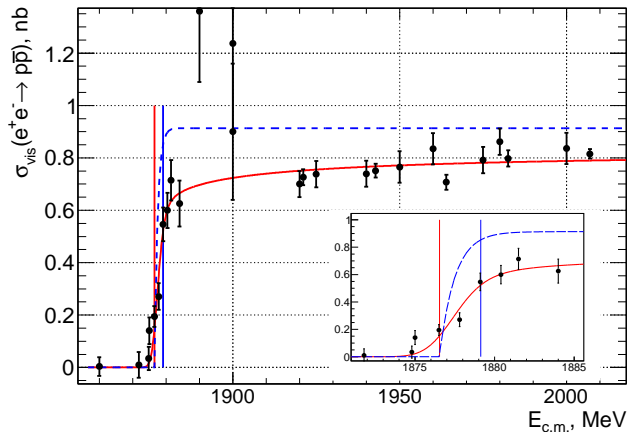


FIG. 3: The $e^+e^- \rightarrow p\bar{p}$ visible cross section measured with the CMD-3 detector. The solid curve shows the result of the fit to an exponentially saturated function (dashed curve) convolved with the 0.95 MeV energy spread and radiation functions. The vertical lines show the $p\bar{p}$ and $n\bar{n}$ thresholds. The inset shows the expanded view of the visible cross section.

V. THE $N\bar{N}$ THRESHOLD REGION

The cross section in Fig. 3 exhibits very sharp step-like behavior close to the $N\bar{N}$ threshold. The Born cross section cannot be obtained without taking into account its smearing due to radiation of real photons by initial electrons and positrons, and the energy spread of the collision energy with $\sigma_{E_{c.m.}} = 0.95 \pm 0.10$ MeV. The vis-

ible cross section is described by a convolution of the radiative cross section, $\sigma_{f\gamma}(E_{c.m.})$, with the c.m. energy spread function:

$$\sigma_{\text{vis}}(E_{c.m.}) = \frac{1}{\sqrt{2\pi}\sigma_{E_{c.m.}}} \int dE'_{c.m.} \sigma_{f\gamma}(E'_{c.m.}) \cdot \exp\left(-\frac{(E_{c.m.} - E'_{c.m.})^2}{2\sigma_{E_{c.m.}}^2}\right), \quad (1)$$

where $\sigma_{f\gamma}(E_{c.m.})$ is a convolution of the Born cross section with the radiator function $F(E_{c.m.}, E_\gamma)$ [28, 29]:

$$\sigma_{f\gamma}(E_{c.m.}) = \int_0^{E_\gamma^{\text{max}}} dE_\gamma \cdot \sigma_{\text{Born}}\left(E_{c.m.} \sqrt{1 - E_\gamma/E_{c.m.}}\right) \cdot F(E_{c.m.}, E_\gamma), \quad (2)$$

where E_γ is the radiative photon energy, and E_γ^{max} is a maximum allowed photon energy for the reaction.

For a demonstration of very fast variation of the cross section, $\sigma_{\text{Born}}(E_{c.m.})$ is described with an exponentially saturated function,

$$\sigma_{\text{Born}}(E_{c.m.}) = A + B \left[1 - \exp\left(-\frac{(E_{c.m.} - E_{\text{thr}})}{\sigma_{\text{thr}}}\right)\right], \quad (3)$$

where E_{thr} ($E_{c.m.} > E_{\text{thr}}$) and σ_{thr} are the energy threshold and a variation scale of the Born cross section, respectively. Parameters A, B are the cross section values below and above the $p\bar{p}$ threshold.

First, the $e^+e^- \rightarrow p\bar{p}$ visible cross section of Fig. 3 is fit to Eq. 3 with all parameters floating except the A value fixed at zero, assuming no signal below the threshold. The fit yields $E_{\text{thr}} = 1877.1 \pm 0.1$ MeV, consistent with the $p\bar{p}$ production threshold within uncertainties in the energy measurement, and $\sigma_{\text{thr}} = 0.18 \pm 0.27$ MeV. Since no $p\bar{p}$ events are expected below the threshold, E_{thr} is fixed at 1876.54 MeV (the doubled proton mass), and the fit yields $\sigma_{\text{thr}} = 0.76 \pm 0.28$ MeV. In both cases the σ_{thr} value and its uncertainty are smaller than the energy difference between the neutron and proton production thresholds. Figure 3 shows the visible $e^+e^- \rightarrow p\bar{p}$ cross section with the fit result. Lines show the $p\bar{p}$ and $n\bar{n}$ threshold positions. An expanded view of the visible $e^+e^- \rightarrow p\bar{p}$ cross section around the $N\bar{N}$ threshold is shown in the inset in Fig. 3.

TABLE I: Results of the fit to the exponentially rising function. Only statistical uncertainties are shown.

Reac.	A, nb	B, nb	E_{thr} , MeV	σ_{thr} , MeV	χ^2/ndf
$p\bar{p}$	0 - fxd	0.91 ± 0.02	1877.1 ± 0.2	0.18 ± 0.27	29/29
$p\bar{p}$	0 - fxd	0.91 ± 0.02	1876.54-fxd	0.76 ± 0.28	31/30
6π	1.55 ± 0.02	-0.42 ± 0.03	1875.8 ± 0.2	0.18 ± 0.67	17/24
6π	1.54 ± 0.02	-0.41 ± 0.03	1876.54-fxd	0.0 ± 2.5	18/25
$2K2\pi$	4.69 ± 0.08	-0.44 ± 0.12	1878.8 ± 0.2	0.35 ± 2.69	7/14
$2K2\pi$	4.70 ± 0.08	-0.45 ± 0.12	1876.54-fxd	2.36 ± 2.01	8/15

Similarly, the $e^+e^- \rightarrow 3(\pi^+\pi^-)$ visible cross section is fit to the above functions with all parameters floating in the energy range $E_{c.m.} = 1835\text{--}1945$ MeV, where the cross section can be considered flat. The fit yields $E_{\text{thr}} = 1875.8 \pm 0.2$ MeV, and $\sigma_{\text{thr}} = 0.18 \pm 0.67$ MeV. The fit with fixed $E_{\text{thr}} = 1876.54$ MeV yields $\sigma_{\text{thr}} = 0.0 \pm 2.5$ MeV, with a good $\chi^2/ndf = 18/25$ value: our statistical accuracy and energy spread allow a drop with a zero width. The result of the latter fit is shown as an inset in Fig. 1 by a solid line, while a dashed line shows the Born cross section. The obtained σ_{thr} value is consistent with that obtained for the $e^+e^- \rightarrow p\bar{p}$ reaction.

Then we fit the $e^+e^- \rightarrow K^+K^-\pi^+\pi^-$ visible cross section to the above functions with all parameters floating in the energy range $E_{c.m.} = 1850\text{--}1970$ MeV, where the cross section can be considered flat. The fit yields $E_{\text{thr}} = 1878.8 \pm 0.2$ MeV: the value is close to the $n\bar{n}$ threshold. The obtained value $\sigma_{\text{thr}} = 0.35 \pm 2.69$ MeV indicates that the observed effect is dominated by the statistical uncertainty, and is consistent with a zero-width drop in the Born cross section. The fit with fixed $E_{\text{thr}} = 1876.54$ MeV yields $\sigma_{\text{thr}} = 2.36 \pm 2.01$ MeV, with a good $\chi^2/ndf = 8/15$ value. The result of the latter fit is shown as an inset in Fig. 2 by a solid line, while a dashed line shows the Born cross section.

The results of the fit are summarized in Table I, and demonstrate that the observed behavior of the cross sections has similar origin, and the ‘‘dip’’ in the hadronic cross section can be interpreted as due to opening of the direct production of the $N\bar{N}$ channel. Note that when the E_{thr} is floating, the obtained value in case of

$3(\pi^+\pi^-)$ is close to the $p\bar{p}$ threshold energy, while for the $K^+K^-\pi^+\pi^-$ channel this value is consistent with the $n\bar{n}$ threshold (1879.13 MeV).

We perform a simultaneous fit of all three channels with common E_{thr} and σ_{thr} values, and the fit yields $1876.87 \pm 0.10 \mp 0.11$ MeV and $0.31 \pm 0.25 \mp 0.15$ MeV, respectively, with $\chi^2/ndf = 66/(67 - 7)$ value. The second uncertainty is systematic and anticorrelated with the systematic uncertainty in the energy spread 0.95 ± 0.10 MeV.

Unfortunately, the accelerator-induced energy spread and relatively low statistical accuracy do not allow us to directly observe a possible structure of this rise (drop) due to the proton-neutron interaction, which could be expected in the studied reactions.

In a recently published paper [13], the authors use the optical potential to make a prediction of the $p\bar{p}$ and $n\bar{n}$ cross section behavior at very small energies above the production thresholds. Figure 4 shows good agreement of available data for the $e^+e^- \rightarrow p\bar{p}$ Born cross section with the theoretical prediction. But for very small deviations from the threshold, energy spread and radiative effects must be taken into account: the result of this convolution for the theoretical function is shown in the inset in comparison with our visible cross section. Note, the suggested model of the final-state interaction of a very slow $N\bar{N}$ pair predicts a nonzero cross section at the $p\bar{p}$ threshold due to the Coulomb interaction, but experimental effects and limited accuracy do not allow us to prove that.

VI. THE $e^+e^- \rightarrow 2(\pi^+\pi^-)$ CROSS SECTION AT THE $N\bar{N}$ THRESHOLD

As suggested in Ref. [13], the total hadronic cross section is strongly affected by virtual production and annihilation of the $N\bar{N}$ pairs. The calculation predicts a 7 nb ‘‘bump’’ in the total cross section (of about 40 nb at this energy), and should be seen in all $e^+e^- \rightarrow \text{hadrons}$ final

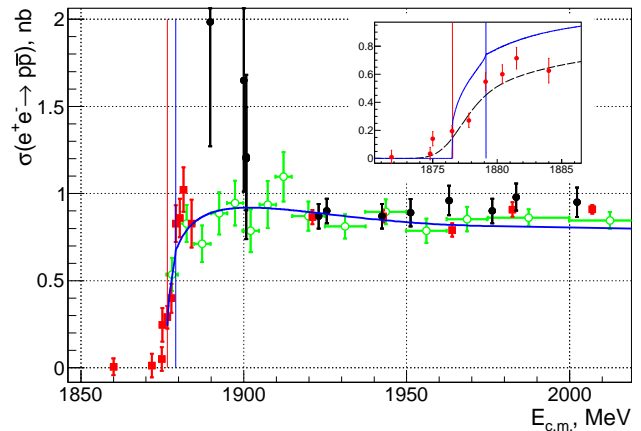


FIG. 4: The $e^+e^- \rightarrow p\bar{p}$ Born cross section measured with CMD-3 (squares) and BaBar (open circles). The solid curve shows the result of the prediction from Refs. [11–13]. The inset shows the expanded view of the visible cross section from CMD-3 with the theoretical prediction for the Born (solid line), and for the visible cross section (dashed line) with the experimental effects. The vertical lines show the $p\bar{p}$ and $n\bar{n}$ thresholds.

states. A naive expectation suggests that the effect could be proportional to the probability of $p\bar{p}$ annihilation into the studied final state.

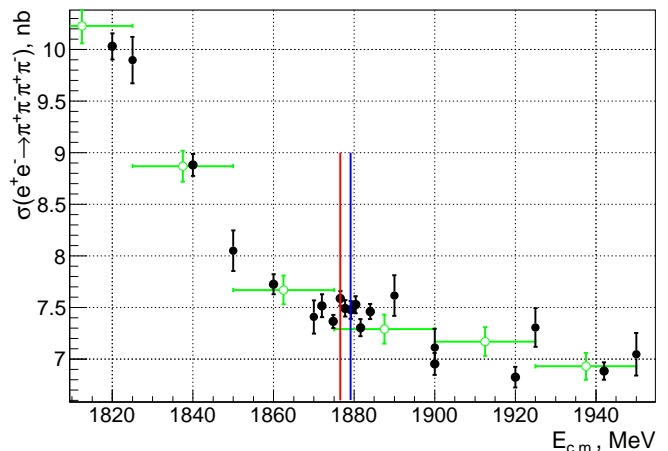


FIG. 5: The $e^+e^- \rightarrow 2(\pi^+\pi^-)$ cross section measured with CMD-3 (dots) and BaBar [31] (open circles). The vertical lines show the $p\bar{p}$ and $n\bar{n}$ thresholds.

To test that, we analyze data at the $N\bar{N}$ threshold by selecting events for the reaction $e^+e^- \rightarrow 2(\pi^+\pi^-)$ according to the procedure described in Ref. [30], and show the obtained cross section in Fig. 5 together with the most

precise measurement by BaBar [31]. No structure exceeding the level of 0.1 nb is observed at the $N\bar{N}$ threshold in either measurement. According to Ref. [32], the $p\bar{p}$ annihilation probability (with isospin one) to four charged pions is about 14%, while for six charged pions it is about 6%. If a cross section drop in the hadronic channel is related to virtual $N\bar{N}$ annihilation [13], for four-pion production one could expect an about 0.5–0.8 nb drop in the cross section, which is not supported by our data. Note that according to Ref. [32] the probability of $N\bar{N}$ annihilation to the $K^+K^-\pi^+\pi^-$ final state is much lower than that for six- or four-pion states, and observation of the “dip” in this channel indicates a complicated production dynamics.

Conclusion

Using the improved performance of VEPP-2000 the scan of the e^+e^- c.m. energy in the 1680 – 2007 MeV range has been performed. A detailed study of the $N\bar{N}$ threshold region confirms a fast drop (rise) in the $e^+e^- \rightarrow 3(\pi^+\pi^-)$ ($e^+e^- \rightarrow p\bar{p}$) cross section observed previously. For the first time a width of this structure is measured in the $e^+e^- \rightarrow p\bar{p}$ reaction: the $\sigma_{\text{thr}} = 0.76 \pm 0.28$ MeV value is smaller than the difference between the $p\bar{p}$ and $n\bar{n}$ production thresholds. The energy position of the “dip” in the $e^+e^- \rightarrow K^+K^-\pi^+\pi^-$ cross sections, observed for the first time, is consistent with the $n\bar{n}$ production threshold, while that for the $e^+e^- \rightarrow 3(\pi^+\pi^-)$ reaction is close to the $p\bar{p}$ threshold. No structures in the $e^+e^- \rightarrow 2(\pi^+\pi^-)$ cross section have been found at the $N\bar{N}$ threshold.

Acknowledgments

The authors are grateful to A. I. Milstein for useful discussions and help with a theoretical interpretation. We thank the VEPP-2000 personnel for excellent machine operation. Part of this work related to the photon reconstruction algorithm in the electromagnetic

calorimeter is supported by the Russian Science Foundation (project #14-50-00080). The work is partially supported by the Russian Foundation for Basic Research grants 16-02-00160-a, 17-02-00327-a, 17-52-50064-a and 18-32-01020. Part of this work related to simulation of multihadronic production is supported by the MSHE grant 14.W03.31.0026.

REFERENCES

- [1] R. Baldini *et al.*, reported at the “Fenice” Workshop, Frascati (1988).
- [2] A. B. Clegg and A. Donnachie, *Z. Phys.* **C45**, 677 (1990).
- [3] M.R. Whalley, *J. Phys.* **G29**, A1 (2003).
- [4] P. L. Frabetti *et al.* (FOCUS Collaboration), *Phys. Lett.* **B514**, 240 (2001).
- [5] P. L. Frabetti *et al.* (FOCUS Collaboration), *Phys. Lett.* **B578**, 290 (2004).
- [6] B. Aubert *et al.* (BaBar Collaboration), *Phys. Rev.* **D73**, 052003 (2006).
- [7] A. Antonelli *et al.* (FENICE Collaboration), *Phys. Lett.* **B365**, 427 (1996).
- [8] R. R. Akhmetshin *et al.* (CMD-3 Collaboration), *Phys. Lett.* **B723**, 82 (2013).
- [9] A. Sibirtsev and J. Haidenbauer, *Phys. Rev.* **D71**, 054010 (2005).
- [10] J. Haidenbauer *et al.*, *Phys. Rev.* **D92**, 054032 (2015).
- [11] V. F. Dmitriev, A. I. Milstein and S. G. Salnikov, *Phys. Rev.* **D93**, 034033 (2016).
- [12] A. I. Milstein, S. G. Salnikov, *Nucl. Phys.* **A966**, 54 (2017).
- [13] A. I. Milstein and S. G. Salnikov, *Nucl. Phys.* **A977**, 60 (2018).
- [14] B. Aubert *et al.* (BaBar Collaboration), *Phys. Rev.* **D73**, 012005 (2006).
- [15] R. R. Akhmetshin *et al.* (CMD-3 Collaboration), *Phys. Lett.* **B759**, 634 (2016).
- [16] M. N. Achasov *et al.* (SND Collaboration), *Phys. Rev.*

- D90, 112007 (2014).
- [17] M. Ablikim *et al.* (BESIII Collaboration), Phys. Rev. Lett. **117**, 042002 (2016).
- [18] B. I. Khazin, Nucl. Phys. B (Proc. Suppl.) **181-182**, 376 (2008).
- [19] V. V. Danilov *et al.*, Proceedings EPAC96, Barcelona, p.1593 (1996).
- [20] I. A. Koop, Nucl. Phys. B (Proc. Suppl.) **181-182**, 371 (2008).
- [21] P. Yu. Shatunov *et al.*, Phys.Part.Nucl.Lett. **13**, 995 (2016).
- [22] D. Shwartz *et al.*, PoS ICHEP2016, 054 (2016).
- [23] E. V. Abakumova *et al.*, Phys. Rev. Lett. **110**, 140402 (2013).
- [24] E. V. Abakumova *et al.*, JINST **10**, T09001 (2015).
- [25] A.E. Ryzhenenkov *et al.*, JINST **12**, C07040 (2017).
- [26] D. N. Shemyakin *et al.*, (CMD-3 Collaboration), Phys. Lett. **B756**, 153 (2016).
- [27] B. Aubert *et al.* (BaBar Collaboration), Phys. Rev. **D76**, 012008 (2007).
- [28] E. A. Kuraev and V. S. Fadin, Sov. J. Nucl. Phys. **41**, 466 (1985).
- [29] S. Actis *et al.*, Eur. Phys. J. **C66**, 585 (2010).
- [30] R. R. Akhmetshin *et al.* (CMD-3 Collaboration), Phys. Lett. **B768**, 345 (2017).
- [31] B. Aubert *et al.*, (BaBar Collaboration), Phys. Rev. **D85**, 112009 (2012).
- [32] E. Klempt, C. Batty, J.-M. Richard, Phys. Rept. **413**, 197 (2005).